

Apsidal motion and absolute parameters for five LMC eccentric eclipsing binaries^{★,★★}

P. Zasche and M. Wolf

Astronomical Institute, Charles University in Prague, Faculty of Mathematics and Physics, 180 00 Praha 8, V Holešovičkách 2, Czech Republic
e-mail: zasche@sirrah.troja.mff.cuni.cz

Received 11 June 2013 / Accepted 15 July 2013

ABSTRACT

Aims. As part of our observational projects at the La Silla Danish 1.54-meter telescope, we aim to measure the precise times of minimum light for eccentric eclipsing binaries in the Large Magellanic Cloud, needed for accurate determination of apsidal motion. Many new times of minima were derived from the photometric databases OGLE and MACHO. Several new minima were also observed. Five early-type and eccentric-orbit eclipsing binaries: HV 982 ($P = 5^d.34$, $e = 0.15$), HV 2274 ($5^d.73$, 0.17), MACHO 78.6097.13 ($3^d.11$, 0.05), MACHO 81.8881.47 ($3^d.88$, 0.22), and MACHO 79.5377.76 ($2^d.64$, 0.06) were studied.

Methods. The O–C diagrams of the systems were analysed using all reliable timings found in the literature, and new or improved elements of apsidal motion were obtained. Light and radial velocity curves of MACHO 81.8881.47 and MACHO 79.5377.76 were analysed using the program PHOEBE.

Results. We derived for the first time or significantly improved the relatively short periods of apsidal motion of 211 (12), 127 (8), 48 (13), 103 (20), and 42 (19) years, respectively. The internal structure constants, $\log k_2$, were found to be -2.37 , -2.47 , -2.17 , -2.02 , and -1.86 respectively, under the assumption that the component stars rotate pseudosynchronously. The relativistic effects are weak, up to 6% of the total apsidal motion rate. The masses for MACHO 81.8881.47 resulted in 5.51 (0.21) and 5.40 (0.19) M_{\odot} , while for MACHO 79.5377.76 the masses are 11.26 (0.35) and 11.27 (0.35) M_{\odot} , respectively.

Key words. binaries: eclipsing – stars: early-type – stars: general – stars: fundamental parameters – Magellanic Clouds

1. Introduction

Eccentric eclipsing binaries (EEB) with an apsidal motion can provide us with an important observational test of theoretical models of stellar structure and evolution. A long-term collecting the times of minima of EEBs observed throughout the apsidal motion cycle and consecutive detailed analysis of the period variations of EEB can be performed, yielding both the orbital eccentricity and the period of rotation of the apsidal line with high accuracy (Giménez 1994). Many different sets of stellar evolution models have been published in recent years, e.g. Maeder (1999), Claret (2004), or Claret (2006); however, to distinguish between them and to test which one is more suitable is still rather difficult. The internal structure constants as derived from the apsidal motion analysis could serve as one independent criterion. On the other hand, to discriminate between the models only stellar parameters for EEBs with an accuracy of 1% can be used.

The Magellanic Clouds are of prime importance in the context of stellar evolution theory. However, the chemical composition of the Magellanic Clouds differs from that of the solar neighborhood (e.g. Ribas 2004) and the study of these massive and metal-deficient stars in the LMC checks our evolutionary models for these abundances. All eclipsing binaries analysed here

have properties that make them important astrophysical laboratories for studying the structure and evolution of massive stars (Ribas 2004).

Here we analyse the observational data and rates of apsidal motion for five LMC detached eclipsing systems. All these systems are early-type objects known to have eccentric orbits and to exhibit apsidal motion. Similar studies of LMC EEBs have been presented by Michalska & Pigulski (2005, hereafter MP05) and Michalska (2007).

2. Observations of minimum light

The monitoring of faint EEBs in external galaxies requires only moderate telescopes in the 1–2 m class range equipped with a modern CCD camera. However, a large amount of observing time is needed, which is unavailable at larger telescopes. During past observational seasons, we accumulated over 1600 photometric observations at selected phases during primary and secondary eclipses and derived 16 precise times of minimum light for selected eccentric systems. New CCD photometry was obtained at the La Silla Observatory in Chile, where the 1.54 m Danish telescope (hereafter DK154) with the CCD camera and RI filters was used.

All CCD measurements were dark-subtracted and then flat-fielded using sky exposures taken at either dusk or dawn. Several comparison stars were chosen in the same frame as the variables. A synthetic aperture photometry and astrometry software developed by Velen and Pravec called APHOT, was routinely used for data obtained. No correction for differential extinction was

* Based on observations made with ESO Telescopes at the La Silla Paranal Observatory under programme ID 68.A-0223(A), and on data collected with the Danish 1.54 m telescope at the ESO La Silla Observatory.

** Appendices are available in electronic form at <http://www.aanda.org>

Table 1. Apical motion elements for HV 982, HV 2274, MACHO 78.6097.13, MACHO 81.8881.47, and MACHO 79.5377.76.

Element [Unit]	HV 982	HV 2274	MACHO 78.6097.13	MACHO 81.8881.47	MACHO 79.5377.76
T_0 [HJD]	2 449 340.5146 (195)	2 448 099.8540(9)	2 452 424.6888 (78)	2 452 282.2431 (178)	2 452 262.6776 (67)
P_s [days]	5.3352210 (97)	5.7259971 (8)	3.1070278 (104)	3.8818717 (32)	2.6365767 (79)
P_a [days]	5.3355902 (97)	5.7267045 (8)	3.1075678 (104)	3.8822732 (33)	2.6370342 (79)
e	0.149 (0.033)	0.1252 (39)	0.0459 (139)	0.217 (23)	0.0574 (160)
$\dot{\omega}$ [deg cycle ⁻¹]	0.0249 (0.0014)	0.0445 (29)	0.0633 (264)	0.03723 (606)	0.0625 (194)
$\dot{\omega}$ [deg yr ⁻¹]	1.705 (0.095)	2.84 (0.20)	7.44 (3.1)	3.50 (0.57)	8.65 (2.68)
ω_0 [deg]	221.2 (0.7)	71.9 (2.9)	27.9 (4.0)	95.9 (8.6)	31.57 (4.20)
U [yr]	211 (12)	126.9 (7.9)	48.4 (12.5)	102.8 (20.0)	41.6 (18.8)

applied because of the proximity of the comparison stars to the variable and the resulting negligible differences in air mass and their similar spectral types.

The new times of primary and secondary minima and their errors were determined by the classical Kwee-van Woerden (1956) algorithm. All new times of minima are given in Table A.1, where epochs are calculated from the ephemeris given in Table 1; the other columns are self-evident.

3. Photometry

For all of the systems we harvested the MACHO (Faccioli et al. 2007) and OGLE (Graczyk et al. 2011) photometry available online. These photometric data were used both for minima times analysis as well as for light curve analysis.

The analysis of the light curves for two of the systems was carried out using the program PHOEBE, ver. 0.31a (Prša & Zwitter 2005), which is based on the Wilson-Devinney algorithm (Wilson & Devinney 1971) and its later modifications, but some of the parameters had to be fixed during the fitting process. The albedo coefficient remained fixed at value 1.0 and the gravity darkening coefficients $g = 1.0$. The limb darkening coefficients were interpolated from the van Hamme tables (van Hamme 1993). A problem emerged with the synchronicity parameters (F_i) due to poor coverage of the RV data near the eclipses and low quality of the light curves used for the LC analysis, hence we fixed these values at $F_i = 0$. The temperature of the primary component was derived from the $V - I$ photometric index, from MP05 and from the resulting masses derived from the combined LC+RV analysis.

4. Spectroscopy

The spectroscopic data for two of the systems (MACHO 81.8881.47, MACHO 79.5377.76) were found in the ESO Archive of the UV-Visual Echelle Spectrograph (UVES) at the Very Large Telescope (VLT). The spectra were obtained during the ESO Period 68 program “*Precise distances to the LMC and SMC from double-lined eclipsing binaries*”; the PI of the project was A. Clausen. Typical exposure times were about 1500 seconds, while the spectra typically have a signal-to-noise ratio (S/N) of about 50. The original data were reduced using the standard ESO routines. The final radial velocities (hereafter RV) used for the analysis were derived via a manual cross-correlation technique (i.e. the direct and flipped profile of spectral lines manually shifted on the computer screen to achieve the best match) using program SPEFO (Horn et al. 1996; Škoda 1996) on several absorption lines in the measured spectral region (usually H_β to H_θ). The derived radial velocities are given in Table B.1. We estimate the error of individual data points to be about 5 km s^{-1} .

5. An approach for the analysis

For the analysis we used the approach presented below. For the systems where the inclination of the orbit is known, the first two steps can be skipped.

- First, all of the available photometric data were analysed, resulting in a set of minima times. Preliminary apical motion parameters were derived (with the assumption $i = 90^\circ$).
- Second, the eccentricity (e), argument of periastron (ω), and apical motion rate ($\dot{\omega}$) derived from the apical motion analysis were used for the preliminary light curve (hereafter LC) analysis.
- Third, the inclination (i) from the LC analysis was used for the final apical motion analysis.
- And finally, the resulting e , ω , and $\dot{\omega}$ values from the apical motion analysis were used for the final LC + RV analysis.

6. Apical motion analysis

The apical motion in all eccentric systems was studied by means of an O–C diagram analysis. All available times of minima, both published in the literature and newly measured, were analysed using the method presented by Giménez & García-Pelayo (1983). This is a weighted least-squares iterative procedure, including terms in the eccentricity up to the fifth order. There are five independent variables (T_0 , P_s , e , $\dot{\omega}$, ω_0) determined in this procedure. The periastron position ω is given by the linear equation

$$\omega = \omega_0 + \dot{\omega} E$$

where $\dot{\omega}$ is the rate of periastron advance, and the position of periastron for the zero epoch T_0 is denoted as ω_0 . The relation between the sidereal and the anomalistic period, P_s and P_a , is given by

$$P_s = P_a (1 - \dot{\omega}/360^\circ),$$

and the period of apical motion by

$$U = 360^\circ P_a / \dot{\omega}.$$

All new precise CCD times of minima were used with a weight of 10 or 20 in our computation. Some of our less precise measurements were weighted by a factor of 5, while the earlier visual and photographic times (esp. the times of the mid-exposure of a photographic plate) were given a weight of one or nought because of the large scatter in these data.

7. Analysis of the systems

7.1. HV 982

The detached eclipsing binary HV 982 (also known as MACHO 82.8043.26, LMCV110; $V_{\max} = 14^m65$; Sp. B5V) is a relatively well-known LMC binary with an eccentric orbit ($e = 0.15$) and a moderate orbital period of 5.3 days. It was discovered to be a variable star by Gaposkin (1970), who published the first photographic light curve.

Pritchard et al. (1994, 1998) in their photometric study derived high surface temperatures (~ 28000 K) and masses ($\sim 8 M_{\odot}$) of components. They also derived the apsidal motion period $U = 205 \pm 7$ years. The precise stellar parameters of components of HV 982 were derived spectroscopically by Fitzpatrick et al. (2002), who found components with similar mass and size,

$$M_1 = 11.28 \pm 0.46 M_{\odot}, M_2 = 11.61 \pm 0.47 M_{\odot}, \\ R_1 = 7.15 \pm 0.12 R_{\odot}, R_2 = 7.92 \pm 0.13 R_{\odot}.$$

The following linear light elements were given in that paper:

$$\text{Pri. Min.} = \text{HJD } 2\,449\,340^d7172 + 5^d33522 \times E.$$

Using the complete analyses of HV 982 they also found the distance to the center of the LMC $d_{\text{LMC}} = 50.7 \pm 1.2$ kpc. Later, Clausen et al. (2003) presented a new accurate CCD *wby* light curve obtained at the Danish 1.54 m telescope at La Silla and derived the precise photometric elements with apsidal motion period $U = 208 \pm 15$ years.

All CCD times of minimum light given in Pritchard et al. (1998) and Clausen et al. (2003) were incorporated into our analysis. Using MACHO (Faccioli et al. 2007) and OGLE (Graczyk et al. 2011) photometry, we were able to derive additional times of minimum light. A total of 68 times of minimum light were used in our analysis (see Table A.1). The orbital inclination adopted was $i = 89^{\circ}.3$, based on the analysis of Fitzpatrick et al. (2002). The computed apsidal motion parameters and their internal errors of the least-squares fit are given in Table 1. In this table, P_s denotes the sidereal period, P_a the anomalistic period, e represents the eccentricity, and $\dot{\omega}$ is the rate of periastron advance (in degrees per cycle and in degrees per year). The zero epoch is given by T_0 , and the corresponding position of the periastron is represented by ω_0 . The O–C residuals for all times of minimum with respect to the linear part of the apsidal motion equation ($\text{Min} = T_0 + P \times E$) are shown in Fig. 1. The non-linear predictions, corresponding to the fitted parameters, are plotted for primary and secondary eclipses.

7.2. HV 2274

The detached and double-lined eclipsing binary HV 2274 (also known as MACHO 19.3577.7, 2MASS J05024076-6824212, LMCV 182, FL 3556; $V_{\max} = 14^m13$; Sp. B1-2 IV-III) is a relatively bright and well-studied LMC eclipsing binary with an eccentric orbit ($e = 0.17$) and a moderate orbital period of 5.7 days. It was discovered to be a variable star by Leavitt (1908). Later, Shapley & Nail (1953) recognized its eclipsing nature and classified it as a β Lyrae type. The eccentric orbit and apsidal motion of HV 2274 was first announced by Watson et al. (1992), who obtained the *BVI_c* CCD photometry at the Mount John University Observatory. See also the history of HV 2274 in the last paper mentioned. Later Claret (1996) found the masses and evolutionary status of this system:

$$\text{Pri. Min.} = \text{HJD } 2\,448\,099^d818 + 5^d726006 \times E.$$

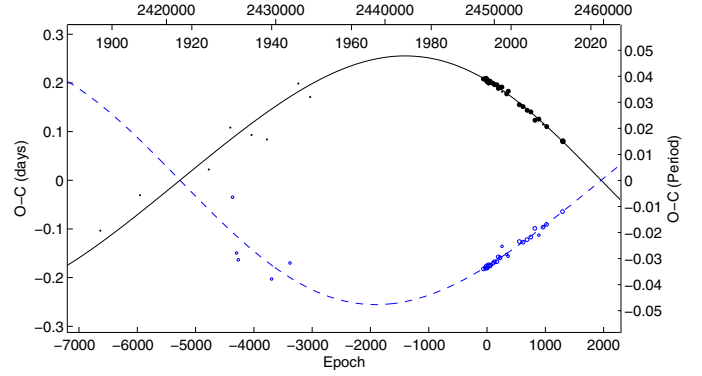


Fig. 1. O–C diagram for the times of minima of HV 982. The continuous and dashed curves represent predictions for the primary and secondary eclipses, respectively. The individual primary and secondary minima are denoted by dots and open circles, respectively. Larger symbols correspond to the photoelectric or CCD measurements that were given higher weights in the calculations.

The fundamental properties of HV 2274 were most recently given in Ribas et al. (2000) who determined the precise absolute parameters of both eclipsing components to be

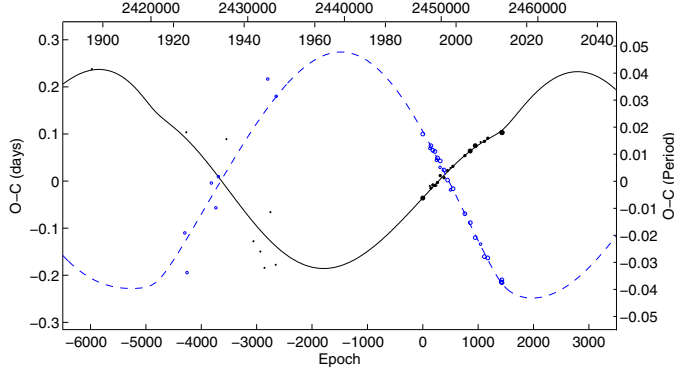
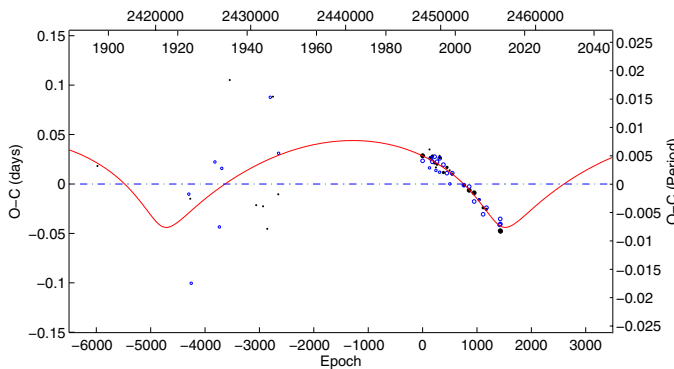
$$M_1 = 12.2 \pm 0.7 M_{\odot}, M_2 = 11.4 \pm 0.7 M_{\odot}, \\ R_1 = 9.86 \pm 0.24 R_{\odot}, R_2 = 9.03 \pm 0.24 R_{\odot}.$$

They also derived the improved apsidal motion period $U = 123 \pm 3$ years and the value of internal structure constant $\log k_{2,\text{obs}} = -2.56$. Since the above-mentioned papers were published, new times of minima have been obtained, which allowed us to reduce the uncertainties in the derived parameters. We collected all times of minimum light given in the literature together with new ones derived from MACHO, OGLE, and our new photometry obtained in Chile. All of these values are listed in Table A.1. In total, 58 precise times of minimum light were used in our analysis, including 29 secondary eclipses. The orbital inclination adopted was $i = 89^{\circ}.6$, based on the analysis of Ribas et al. (2000).

Analysing the available data using the apsidal motion hypothesis, we found an additional variation superimposed on the apsidal motion. Hence, we used a different code computing the apsidal motion parameters together with the third-body orbit (a so-called light travel time effect), see e.g. Irwin (1959). Altogether, ten parameters were fitted (five from apsidal motion, five from the third body hypothesis), thus this approach led to an acceptable solution. The resulting parameters of the fit are given in Tables 1 and 2, the complete O–C diagrams are shown in Figs. 2 and 3. From the third-body parameters we were also able to compute the mass function of the distant component, which resulted in $f(m_3) = 0.053 \pm 0.008 M_{\odot}$. From this value, we calculated the predicted minimal mass of the third body (i.e. assuming coplanar orbits $i_3 = 90^{\circ}$), which resulted in $m_{3,\text{min}} = 3.4 M_{\odot}$. If we propose this body in the system, one can ask whether it is detectable somehow in the already-obtained data. The period is rather long for continuous monitoring of the radial velocity changes, but detecting the third light in the light curve solution is difficult. Assuming a normal main sequence star, its luminosity is about only 1% of the total system luminosity. Such a weak third light could be detectable only in extremely precise photometric data for the light curve solution.

Table 2. Third-body orbit parameters for HV 2274.

Element [Unit]	Value
p_3 [yr]	98.2 ± 14.3
A_3 [day]	0.045 ± 0.009
T_3 [HJD]	$2\,456\,205 \pm 5033$
e_3	0.654 ± 0.047
ω_3 [deg]	251.1 ± 7.1


Fig. 2. O–C diagram for the times of minima of HV 2274. See legend to Fig. 1. The final fit is composed from two effects: the apsidal motion together with the third-body hypothesis.

Fig. 3. O–C residuals for HV 2274 after subtraction of the apsidal motion term. Only the third body effect is plotted.

7.3. MACHO 78.6097.13

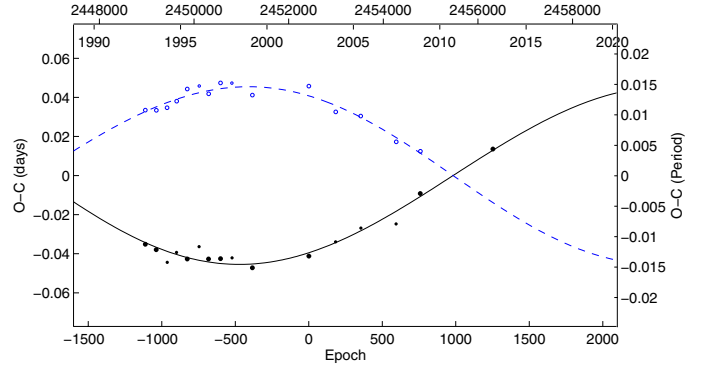
The detached eclipsing binary MACHO 78.6097.13 (also known as OGLE J051804.81-694818.9, LMC MP#5; $V_{\max} = 14^m37$, sp O9V+O9V) is an eccentric binary system ($e = 0.046$) with a short orbital period ($P = 3.1$ d) discovered by MP05 in the OGLE field LMC-SC7.

Our analysis gives the following ephemeris:

$$\text{Pri. Min.} = \text{HJD } 2\,452\,424^d6888 + 3^d1070278 \times E.$$

The most detailed analysis of the system was published by González et al. (2005), which was based on the ESO spectral observations together with the MACHO data. They also derived the masses and radii of both components that were used in the present analysis. Both components are of O9 spectral types, which makes this system the earliest in our sample.

Our new times of minimum light, as well as the timings derived from MACHO and OGLE photometry are given in Table A.1. All of these data (31 minima times) were used in our calculations. Using the parameters presented by González et al. (2005),


Fig. 4. O–C graph for the times of minimum of MACHO 78.6097.13. See legend to Fig. 1.

we analysed the system on apsidal motion, deriving the parameters given in Table 1. As one can see, this system has the lowest eccentricity in our sample and the apsidal advance is rather fast: almost one half of the period has been covered with observations so far.

7.4. MACHO 81.8881.47

The detached eclipsing binary MACHO 81.8881.47 (also known as OGLE J053517.75-694318.7, LMC MP#7; $V_{\max} = 14^m9$; Sp. B) is a relatively bright binary system with an eccentric orbit ($e = 0.2$) and a moderate orbital period $P \approx 3.9$ days. Its variability was discovered by MP05 in the OGLE field LMC-SC16. Most recently, Graczyk et al. (2011) included this star in their catalogue of eclipsing binaries in the LMC. They also gave the preliminary ephemeris:

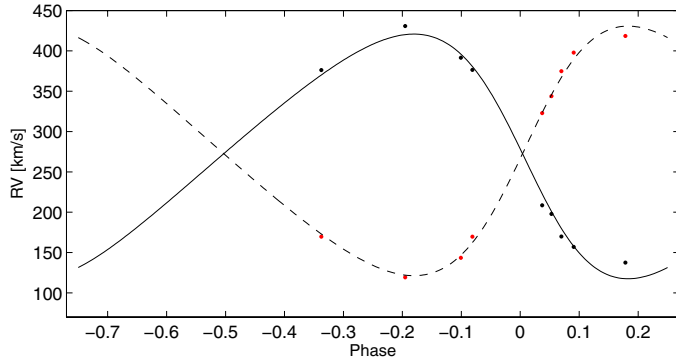
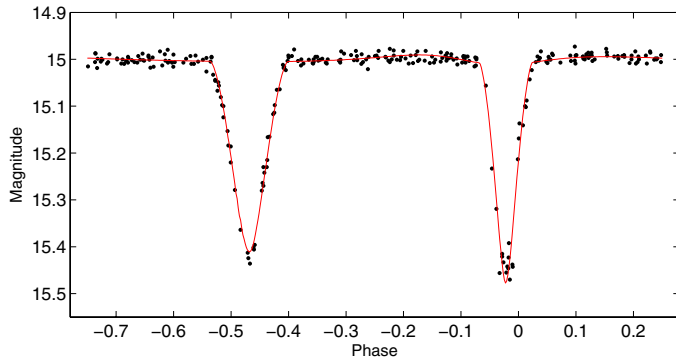
$$\text{Pri. Min.} = \text{HJD } 2\,453\,571^d1063 + 3^d881980 \times E.$$

Using OGLE and MACHO photometry, we were also able to derive additional times of minimum light; two more minima were derived from our observations. Only 30 times of minimum light were used in our analysis (see Table A.1). As one can clearly see from the shape of the light curve and the different duration of both the primary and secondary eclipse, this is the system with the highest value of eccentricity in our sample.

We used the ESO data for deriving the radial velocities of the components. Ten UVES spectra were found, of which nine were usable for the analysis. The derived RVs of both components are given in Table B.1. Together with these radial velocities, the MACHO light curve was used for the subsequent combined LC+RV analysis. The final parameters of the solution are given in Table 3, while the fits are plotted in Figs. 5 and 6. Our results show the rather noticeable property that the more massive component (the primary) is smaller and less luminous (i.e. has a lower temperature). However, this is still a preliminary result based on only nine RVs and a poor fit. Although the scenario is possible, the more probable explanation is that the mass ratio is inverse, and the primary and secondary components are interchanged. This can be allowed for within the uncertainties of the mass ratio. A more detailed analysis is needed, based on more precise spectral observations. The orbital inclination was about $i = 84.2^\circ$, which was later used for the apsidal motion analysis. The resulting parameters of apsidal motion are found in Table 1, and the current O–C diagram is shown in Fig. 7. As one can see, the period is rather long and only about 1/5 has been covered so far.

Table 3. Light and radial velocity curve fit parameters for MACHO 81.8881.47 and MACHO 79.5377.76.

Parameter	MACHO 81.8881.47	MACHO 79.5377.76
T_1 [K]	17 200 (fixed)	27 500 (fixed)
T_2 [K]	18 420 (360)	26 710 (470)
i [deg]	84.20 (0.27)	87.22 (0.44)
Ω_1	7.067 (0.115)	5.774 (0.085)
Ω_2	6.365 (0.102)	6.264 (0.098)
$q = M_2/M_1$	0.981 (0.030)	1.00 (0.02)
a [R_\odot]	23.04 (0.12)	22.65 (0.07)
v_γ [km s^{-1}]	272.6 (1.6)	250.0 (1.0)
L_1 [%]	41.4 (1.2)	57.2 (1.5)
L_2 [%]	58.6 (1.4)	42.8 (1.1)

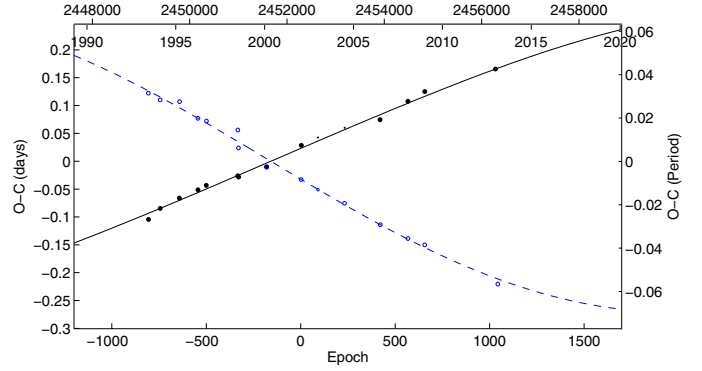
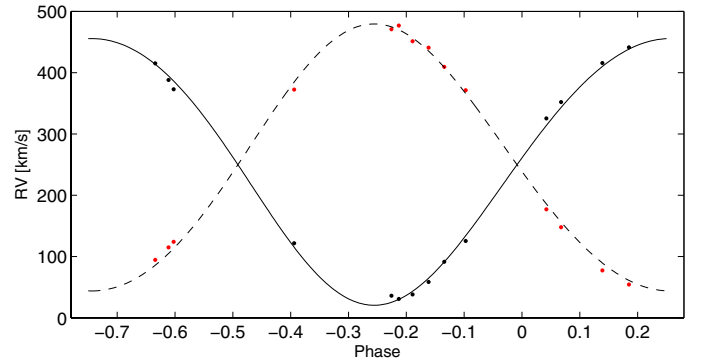
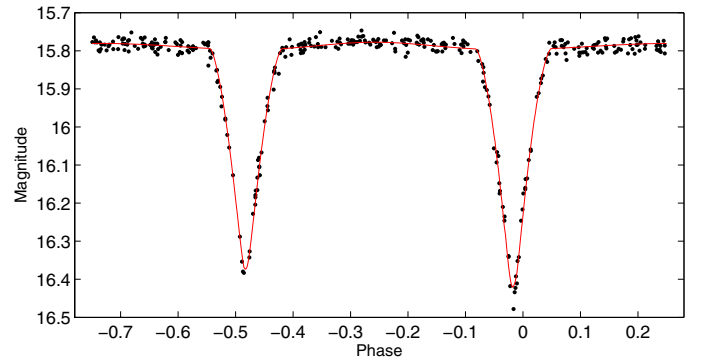

Fig. 5. Radial velocity curve for MACHO 81.8881.47.

Fig. 6. Light curve for MACHO 81.8881.47.

7.5. MACHO 79.5377.76

The detached eclipsing binary MACHO 79.5377.76 (also known as OGLE J051323.98-692249.2, $V_{\text{max}} = 15^m8$; Sp. B) is a fairly neglected binary system with a moderate eccentric orbit ($e = 0.06$) and a short orbital period ($P \approx 2.64$ day):

$$\text{Pri. Min.} = \text{HJD } 2\,452\,262^d.6776 + 2^d.6365767 \times E.$$

We used the MACHO and OGLE photometry together with our new observations from Chile to derive the times of minima, the ESO spectral observations to derive the radial velocities, and the MACHO photometry to model the light curve of the system. Our results are plotted in Figs. 8 and 9. The resulting parameters are given in Table 3. As one can see, both components are of equal mass and their spectral type was estimated to be about B0-B1. Radial velocities used for our analysis are also given in Table B.1. The coverage of the radial velocity curve is better than for MACHO 81.8881.47; however, it was rather difficult to


Fig. 7. O-C graph of MACHO 81.8881.47. See legend for Fig. 1.

Fig. 8. Radial velocity curve for MACHO 79.5377.76.

Fig. 9. Light curve for MACHO 79.5377.76.

derive the synchronicity parameters F_i , and so we fixed them at $F_i = 0$. A total of 34 reliable times of minimum light were used in our analysis including 16 secondary eclipses (see tables in the Appendices). The final apsidal motion elements are given in Table 1, and the O-C graph is shown in Fig. 10. The apsidal period is the shortest among systems studied here, only 42 years.

8. Discussion

The detection of apsidal motion in EEB provides the opportunity to test models of stellar internal structure. The internal structure constant (ISC) $k_{2,\text{obs}}$ is related to the variation in the density inside the star and can be derived using the expression

$$k_{2,\text{obs}} = \frac{1}{c_{21} + c_{22}} \frac{P_a}{U} = \frac{1}{c_{21} + c_{22}} \frac{\dot{\omega}}{360}, \quad (1)$$

Table 4. Basic physical properties of HV 982, HV 2284, MACHO 78.6097.13, MACHO 81.8881.47, and MACHO 79.5377.76 and their internal structure constants.

Parameter	Unit	HV 982	HV 2274	MACHO 78.6097.13	MACHO 81.8881.47	MACHO 79.5377.76
M_1	M_\odot	11.28 (0.46)	12.2 (0.7)	11.76 (0.48)	5.51 (0.21)	11.26 (0.35)
M_2	M_\odot	11.61 (0.47)	11.4 (0.7)	10.51 (0.40)	5.40 (0.19)	11.27 (0.35)
r_1		0.194 (0.003)	0.255 (0.013)	0.258 (0.021)	0.169 (0.008)	0.212 (0.004)
r_2		0.214 (0.003)	0.234 (0.012)	0.206 (0.020)	0.192 (0.010)	0.190 (0.004)
Source		Clausen et al. (2003)	Ribas et al. (2000)	González et al. (2005)	This paper	This paper
$\dot{\omega}_{\text{rel}}$	deg cycle ⁻¹	0.0015	0.0014	0.0020	0.0011	0.0023
$\dot{\omega}_{\text{rel}}/\dot{\omega}$	%	5.9	3.2	3.24	3.06	3.65
$\log k_{2,\text{obs}}$		-2.371 (0.10)	-2.470 (0.15)	-2.174 (0.35)	-2.017 (0.18)	-1.859 (0.17)
$\log k_{2,\text{theo}}$		-2.32	-2.45	-2.19	-2.01	-1.90

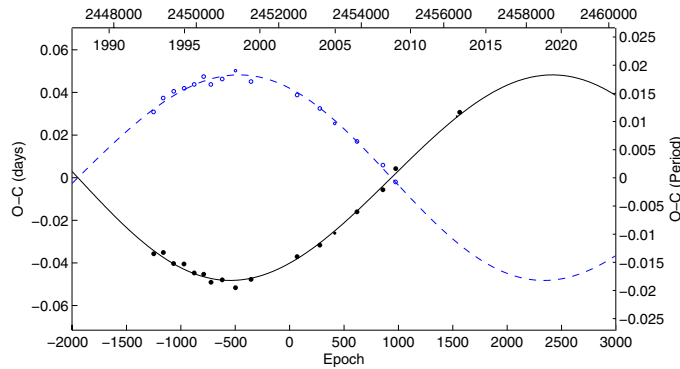


Fig. 10. O-C diagram for MACHO 79.5377.76. See legend to Fig. 1.

where c_{21} and c_{22} are functions of the orbital eccentricity, fractional radii, the masses of the components, and the ratio between rotational velocity of the stars and Keplerian velocity (Kopal 1978). We also assume that the component stars rotate pseudosynchronously with the same angular velocity as the maximum orbital value at periastron (see e.g. Kopal 1978). Another possible approach is to use the value of $v \sin i$ as derived from the combined LC+RV analysis published earlier. However, there could be a problem with the inclination of the rotation axis (as in the case of DI Her) and, moreover, the error of the internal structure constants is by far dominated by the term r_i^5 in the equations. In addition to the classical Newtonian contribution, the observed rate of rotation of the apses includes the contribution from General Relativity (Giménez 1985),

$$\dot{\omega}_{\text{rel}} = 5.45 \times 10^{-4} \frac{1}{1 - e^2} \left(\frac{M_1 + M_2}{P} \right)^{2/3}, \quad (2)$$

where M_i denotes the individual masses of the components in solar units and P is the orbital period in days.

The values of $\dot{\omega}_{\text{rel}}$ and the resulting mean internal structure constants $k_{2,\text{obs}}$ for the systems studied are given in Table 4. Theoretical values $k_{2,\text{theo}}$ according to available theoretical models for the internal stellar structure computed by Claret (2006) for given masses of components are presented in Table 4.

We tried to compare our resulting systemic velocities with other published values of eclipsing binaries in the LMC, see Table 5 and Fig. 11. There are still only a few such systems studied in detail (i.e. LC+RV analysis). Therefore, reliable analysis of different velocities within the LMC is still very difficult. We can only compare our Fig. 11 with other kinematic studies of the LMC published earlier, e.g. that by Reid & Parker (2006)

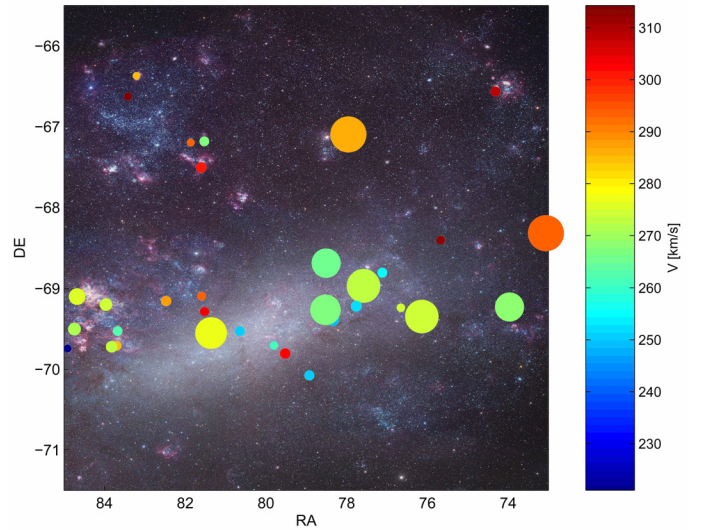


Fig. 11. Position and systemic velocities (see the colour scale on the right) of eclipsing binaries located in the LMC and its vicinity, see Table 5. The larger the symbol, the higher the precision. The background image of the LMC is used with the permission of the author Robert Gendler (<http://www.robgendlerastropics.com>).

or Rohlfs et al. (1984), that were based on much larger radial-velocity data sets. Nevertheless, we can conclude that our two new systemic velocities roughly fit the overall picture and the total velocity dispersion within the LMC is more than 30 km s^{-1} .

9. Conclusions

The apsidal motion in EEB has been used for decades to test evolutionary stellar models. This study provides accurate information on the apsidal motion rates of five main-sequence early-type binary systems in the LMC: HV 982, HV 2274, MACHO 78.6097.13, MACHO 81.8881.47, and MACHO 79.5377.76. In our Galaxy there are known a few hundreds of apsidal motion EEBs, however in the LMC there are still only a few dozen of these systems (Michalska & Pigulski 2005). Hence this study still presents an important contribution to the topic. The relativistic effects are weak, being up to 6% of the total apsidal motion rate. For the systems MACHO 79.5377.76 and MACHO 81.8881.47, their light and radial velocity curves were analysed for the first time yielding the stellar parameters of both components given in Table 4. Moreover, when the MACHO 79.5377.76 internal structure constant and the

Table 5. Radial velocities of eclipsing binaries in the LMC derived from various analyses.

System	RA [h m s]	DE [° ' "]	<i>P</i> [d]	RV [km s ⁻¹]	Reference
MACHO 47.1884.17	04 52 15.29	-68 19 10.55	251.0068	293.44 ± 0.04	Pietrzyński et al. (2013)
MACHO 18.2475.67	04 55 51.48	-69 13 47.99	150.0198	267.68 ± 0.08	Pietrzyński et al. (2013)
HV 2241	04 57 15.74	-66 33 54.20	4.342635	307.9 ± 3	Ostrov et al. (2001)
HV 2274	05 02 40.80	-68 24 21.02	5.726006	312 ± 4	Ribas et al. (2000)
MACHO 1.3926.29	05 04 32.88	-69 20 50.99	189.8215	274.32 ± 0.05	Pietrzyński et al. (2013)
MACHO 1.4290.113	05 06 37.80	-69 14 22.98	2.273210	274.2 ± 4.5	González et al. (2005)
MACHO 1.4539.37	05 08 28.10	-68 48 26.02	2.995450	255.6 ± 3.1	González et al. (2005)
OGLE LMC-ECL-9114	05 10 19.65	-68 58 12.0	214.1707	272.04 ± 0.05	Pietrzyński et al. (2013)
MACHO 79.5017.83	05 11 02.80	-69 13 09.01	2.152915	252.0 ± 2.0	González et al. (2005)
MACHO 52.5169.24	05 11 49.45	-67 05 45.20	167.6350	286.24 ± 0.04	Pietrzyński et al. (2013)
MACHO 79.5377.76	05 13 23.91	-69 22 48.90	2.636577	250.0 ± 1.0	This paper
MACHO 2.5509.50	05 14 01.91	-68 41 18.41	117.8708	265.10 ± 0.08	Pietrzyński et al. (2013)
MACHO 79.5500.60	05 14 05.95	-69 15 56.83	771.7806	266.38 ± 0.07	Pietrzyński et al. (2013)
MACHO 6.5730.3092	05 15 41.50	-70 04 39.00	1.761014	250.9 ± 2.6	González et al. (2005)
MACHO 78.6097.13	05 18 04.70	-69 48 19.02	3.107023	301.7 ± 2.4	González et al. (2005)
HV 12012	05 19 11.78	-69 42 24.38	2.727125	261.4 ± 4.6	Ribas et al. (2002)
MACHO 78.6827.66	05 22 35.00	-69 31 44.01	2.183358	250.8 ± 3.0	González et al. (2005)
MACHO 77.7311.102	05 25 25.55	-69 33 04.49	157.3243	276.66 ± 0.06	Pietrzyński et al. (2013)
MACHO 80.7436.52	05 26 04.40	-69 17 10.99	1.664135	303.2 ± 3.8	González et al. (2005)
TYC 8891-3349-1	05 26 06.15	-67 10 56.98	3.30161	267 ± 3	Ostrov & Lapasset (2003)
MACHO 80.7438.42	05 26 21.60	-69 05 45.00	1.505947	292.7 ± 4.4	González et al. (2005)
[L72] LH 54-425	05 26 24.25	-67 30 17.19	2.24741	300.9 ± 2.3	Williams et al. (2008)
HV 2543	05 27 27.40	-67 11 54.55	4.829046	293.2 ± 6	Ostrov et al. (2000)
HV 982	05 29 53.00	-69 09 22.99	5.335220	287.8 ± 2.5	Fitzpatrick et al. (2002)
LMC X-4	05 32 49.54	-66 22 13.30	1.40830	284.0 ± 7.0	Hutchings et al. (1978)
HV 5936	05 33 39.03	-66 37 39.61	2.805068	314.3 ± 5.8	Fitzpatrick et al. (2003)
MACHO 81.8881.21	05 34 48.14	-69 42 36.30	4.250806	284 ± 3	Bonanos (2009)
MACHO 81.8763.8	05 34 41.30	-69 31 39.01	1.404740	263.1 ± 3	Ostrov (2001)
MACHO 81.8881.47	05 35 17.57	-69 43 18.90	3.881872	272.6 ± 1.6	This paper
MACHO 82.9010.36	05 35 50.79	-69 12 00.44	2.762456	273.8 ± 1.2	Massey et al. (2012)
[HSH95] 38	05 38 42.10	-69 06 07.79	3.39	275.3 ± 0.5	Massey et al. (2002)
[HSH95] 39	05 38 42.49	-69 06 01.29	4.06	266.9 ± 0.5	Massey et al. (2002)
[HSH95] 42	05 38 42.18	-69 06 02.38	2.89	272.0 ± 0.5	Massey et al. (2002)
[HSH95] 77	05 38 42.56	-69 06 04.39	1.88	275.2 ± 0.5	Massey et al. (2002)
LMC X-3	05 38 56.63	-64 05 03.30	1.7049	310.0 ± 7.0	Cowley et al. (1983)
[M2002] LMC 172231	05 38 58.10	-69 30 11.31	3.225414	271.5 ± 1.2	Massey et al. (2012)
LMC X-1	05 39 38.84	-69 44 35.70	4.2288	221.0 ± 6.0	Hutchings et al. (1987)

theoretical model are compared the system appears to be very young ($\sim 2 \times 10^6$ yr).

In spite of the considerable amount of observational data that has been collected for decades, the absolute dimensions of massive binary components are only known with an accuracy of about 1–3% (e.g. Clausen 2004). More detailed study based on more precise radial velocities would be very profitable to derive the physical properties of components with higher accuracy. The most promising system for further detailed analysis seems to be HV 2274 because of the putative third component in the system. We still know only a few such systems nowadays, see e.g. Bozkurt & Değirmenci (2007), while HV 2274 is the first to be discovered out of our Galaxy. Only precise spectral observations and their disentangling should reveal its true nature.

Acknowledgements. We do thank the MACHO and OGLE teams for making all of the observations easily and publicly available. This work was supported by the Research Program MSM0021620860 *Physical Study of objects and processes in the Solar System and in Astrophysics* of the Ministry of Education of the Czech Republic, by the Czech Science Foundation grant no. P209/10/0715, by the grant UNCE 12 of the Charles University in Prague, and by the grant LG12001 of the Ministry of Education of the Czech Republic. We are also grateful to the ESO team at the La Silla Observatory for their help in maintaining and operating the Danish telescope. The authors would like to thank M. Zejda, J. Liška, J. Janík, and M. Skarka for their important help with photometric observations. G. Michalska is also acknowledged for sending us the unpublished times

of minima for selected binaries. The following internet-based resources were used in research for this paper: the SIMBAD database and the VizieR service operated at the CDS, Strasbourg, France, the NASA Astrophysics Data System Bibliographic Services, and the ESO Science Archive Facility.

References

- Bonanos, A. Z. 2009, *ApJ*, 691, 407
Bozkurt, Z., & Değirmenci, Ö. L. 2007, *MNRAS*, 379, 370
Claret, A. 1996, *A&A*, 315, 415
Claret, A. 2004, *A&A*, 424, 919
Claret, A. 2006, *A&A*, 453, 769
Clausen, J. V. 2004, *New Astron. Rev.*, 48, 679
Clausen, A., Storm, J., Larsen, S. S., & Giménez, A. 2003, *A&A*, 402, 509
Cowley, A. P., Crampton, D., Hutchings, J. B., Remillard, R., & Penfold, J. E. 1983, *ApJ*, 272, 118
Faccioli, L., Alcock, C., Cook, K., et al. 2007, *AJ*, 134, 1963
Fitzpatrick, E. L., Ribas, I., Guinan, E. F., et al. 2002, *ApJ*, 564, 260
Fitzpatrick, E. L., Ribas, I., Guinan, E. F., Maloney, F. P., & Claret, A. 2003, *ApJ*, 587, 685
Gaposhkin, S. 1970, *SAO Special Report*, 310
Gaposhkin, S. I. 1977, *SAO Special Report*, 380
Giménez, A. 1985, *ApJ*, 297, 405
Giménez, A. 1994, *Exp. Astron.*, 5, 91
Giménez, A., & García-Pelayo, J. M. 1983, *Ap&SS*, 92, 203
González, J. F., Ostrov, P., Morrell, N., & Minniti, D. 2005, *ApJ*, 624, 946
Graczyk, D., Soszyński, I., Poleski, R., et al. 2011, *AcA*, 61, 103
Horn, J., Kubát, J., Harmanec, et al. 1996, *A&A*, 309, 521
Hutchings, J. B., Crampton, D., & Cowley, A. P. 1978, *ApJ*, 225, 548

- Hutchings, J. B., Crampton, D., Cowley, A. P., Bianchi, L., & Thompson, I. B. 1987, *AJ*, 94, 340
- Irwin, J. B. 1959, *AJ*, 64, 149
- Kopal, Z. 1978, *Dynamics of Close Binary Systems* (Dordrecht: Reidel), *Astrophys. Space Sci. Lib.*, 68, 524
- Kwee, K. K., & van Woerden, H. 1956, *Bull. Astron. Inst. Netherlands*, 12, 327
- Leavitt, H. S. 1908, *Annals of Harvard College Observatory*, 60, 87
- Massey, P., Penny, L. R., & Vukovich, J. 2002, *ApJ*, 565, 982
- Massey, P., Morrell, N. I., Neugent, K. F., et al. 2012, *ApJ*, 748, 96
- Maeder, A. 1999, *A&A*, 347, 185
- Michalska, G. 2007, *IBVS No. 5759*
- Michalska, G., & Pigulski, A. 2005, *A&A*, 434, 89
- Ostrov, P. G. 2001, *MNRAS*, 321, L25
- Ostrov, P. G., & Lapasset, E. 2003, *MNRAS*, 338, 141
- Ostrov, P. G., Lapasset, E., & Morrell, N. I. 2000, *A&A*, 356, 935
- Ostrov, P. G., Morrell, N. I., & Lapasset, E. 2001, *A&A*, 377, 972
- Pietrzyński, G., Graczyk, D., Gieren, W., et al. 2013, *Nature*, 495, 76
- Pritchard, J. D., Tobin, W., & Clark, M. 1994, *Exp. Astron.*, 5, 43
- Pritchard, J. D., Tobin, W., Clark, M., & Guinan, E. F. 1998, *MNRAS*, 299, 1087
- Prša, A., & Zwitter, T. 2005, *ApJ*, 628, 426
- Reid, W. A., & Parker, Q. A. 2006, *MNRAS*, 373, 521
- Ribas, I. 2004, *New Astron. Rev.*, 48, 731
- Ribas, I., Guinan, E. F., Fitzpatrick, E. L. et al. 2000, *ApJ*, 528, 692
- Ribas, I., Fitzpatrick, E. L., Maloney, F. P., Guinan, E. F., & Udalski, A. 2002, *ApJ*, 574, 771
- Rohlf, K., Kreitschmann, J., Feitzinger, J. V., & Siegmán, B. C. 1984, *A&A*, 137, 343
- Shapley, H., & Nail, V. McK. 1953, *Proc. Nat. Acad. Sci.*, 39, 1
- Škoda, P. 1996, in *Astronomical Data Analysis Software and Systems V*, eds. G. H. Jacoby, & J. Barnes, *ASP Conf. Ser.*, 101, 187
- van Hamme, W. 1993, *AJ*, 106, 2096
- Watson, R. D., West, S. R. D., Tobin, W., & Gilmore, A. C. 1992, *MNRAS*, 528, 527
- Williams, S. J., Gies, D. R., Henry, T. J., et al. 2008, *ApJ*, 682, 492
- Wilson, R. E., & Devinney, E. J. 1971, *ApJ*, 166, 605
- Wozniak, P. R., Vestrand, W. T., Akerlof, C. W., et al. 2004, *AJ*, 127, 2436

Appendix A: Table of minima

Table A.1. List of the minima timings used for the analysis.

Star	JD Hel.- 2 400 000	Error [day]	Epoch	Filter	Source Observatory
HV 982	13 946.555	0.05	-6634.0		Gaposhkin (1977)
HV 982	17 590.584	0.05	-5951.0		Gaposhkin (1977)
HV 982	23 875.527	0.05	-4773.0		Gaposhkin (1977)
HV 982	25 849.645	0.05	-4403.0		Gaposhkin (1977)
HV 982	26 060.243	0.10	-4363.5		Gaposhkin (1977)
HV 982	26 412.253	0.05	-4297.5		Gaposhkin (1977)
HV 982	26 577.631	0.05	-4266.5		Gaposhkin (1977)
HV 982	27 786.315	0.05	-4040.0		Gaposhkin (1977)
HV 982	29 189.469	0.10	-3777.0		Gaposhkin (1977)
HV 982	29 629.338	0.05	-3694.5		Gaposhkin (1977)
HV 982	31 304.630	0.05	-3380.5		Gaposhkin (1977)
HV 982	32 070.603	0.05	-3237.0		Gaposhkin (1977)
HV 982	33 153.625	0.05	-3034.0		Gaposhkin (1977)
HV 982	49 335.3866	0.0004	-1.0	<i>wby</i> VI	Pritchard et al. (1998)
HV 982	49 337.6668	0.0004	-0.5	<i>wby</i> VI	Pritchard et al. (1998)
HV 982	49 337.6670	0.0010	-0.5	<i>wby</i>	Clausen et al. (2003)
HV 982	49 340.7172	0.0005	0.0	<i>wby</i>	Clausen et al. (2003)
HV 982	50 695.852	0.11	254.0	<i>wby</i> VI	Pritchard et al. (1998)
HV 982	49 186.00052	0.01299	-29.0	<i>R</i>	MACHO, this paper
HV 982	49 188.28011	0.00421	-28.5	<i>R</i>	MACHO, this paper
HV 982	49 618.14725	0.00256	52.0	<i>R</i>	MACHO, this paper
HV 982	49 620.43922	0.01275	52.5	<i>R</i>	MACHO, this paper
HV 982	50 023.61929	0.00560	128.0	<i>R</i>	MACHO, this paper
HV 982	50 025.92309	0.00405	128.5	<i>R</i>	MACHO, this paper
HV 982	50 370.40101	0.00352	193.0	<i>R</i>	MACHO, this paper
HV 982	50 367.38712	0.00629	192.5	<i>R</i>	MACHO, this paper
HV 982	50 711.84825	0.02668	257.0	<i>R</i>	MACHO, this paper
HV 982	50 714.19804	0.02646	257.5	<i>R</i>	MACHO, this paper
HV 982	51 277.38263	0.01014	363.0	<i>R</i>	MACHO, this paper
HV 982	51 279.71120	0.03201	363.5	<i>R</i>	MACHO, this paper
HV 982	49 020.60964	0.00588	-60.0	<i>B</i>	MACHO, this paper
HV 982	49 017.55154	0.00615	-60.5	<i>B</i>	MACHO, this paper
HV 982	49 260.69563	0.00240	-15.0	<i>B</i>	MACHO, this paper
HV 982	49 262.97768	0.00197	-14.5	<i>B</i>	MACHO, this paper
HV 982	49 490.10034	0.00331	28.0	<i>B</i>	MACHO, this paper
HV 982	49 487.05952	0.00848	27.5	<i>B</i>	MACHO, this paper
HV 982	49 612.81440	0.00315	51.0	<i>B</i>	MACHO, this paper
HV 982	49 609.76750	0.00955	50.5	<i>B</i>	MACHO, this paper
HV 982	49 879.57123	0.002614	101.0	<i>B</i>	MACHO, this paper
HV 982	49 881.86935	0.00480	101.5	<i>B</i>	MACHO, this paper
HV 982	50 231.69273	0.00384	167.0	<i>B</i>	MACHO, this paper
HV 982	50 233.99656	0.004588	167.5	<i>B</i>	MACHO, this paper
HV 982	50 530.45942	0.00416	223.0	<i>B</i>	MACHO, this paper
HV 982	50 532.77709	0.00219	223.5	<i>B</i>	MACHO, this paper
HV 982	51 133.32646	0.00331	336.0	<i>B</i>	MACHO, this paper
HV 982	51 135.66413	0.00742	336.5	<i>B</i>	MACHO, this paper
HV 982	52 293.43371	0.01771	553.5	<i>I</i>	OGLE, this paper
HV 982	52 291.04698	0.03068	553.0	<i>I</i>	OGLE, this paper
HV 982	52 632.49722	0.00320	617.0	<i>I</i>	OGLE, this paper
HV 982	52 634.88640	0.00213	617.5	<i>I</i>	OGLE, this paper
HV 982	53 005.95515	0.00261	687.0	<i>I</i>	OGLE, this paper
HV 982	53 008.35696	0.00726	687.5	<i>I</i>	OGLE, this paper
HV 982	53 355.15161	0.00636	752.5	<i>I</i>	OGLE, this paper
HV 982	53 358.07636	0.01552	753.0	<i>I</i>	OGLE, this paper
HV 982	53 720.85428	0.01008	821.0	<i>I</i>	OGLE, this paper
HV 982	53 717.96464	0.02203	820.5	<i>I</i>	OGLE, this paper
HV 982	54 083.65165	0.01595	889.0	<i>I</i>	OGLE, this paper
HV 982	54 086.08062	0.03	889.5	<i>I</i>	OGLE, this paper
HV 982	54 462.44122	0.02	960.0	<i>I</i>	OGLE, this paper
HV 982	54 464.89826	0.00320	960.5	<i>I</i>	OGLE, this paper
HV 982	54 793.22040	0.00373	1022.0	<i>I</i>	OGLE, this paper
HV 982	54 790.35208	0.00774	1021.5	<i>I</i>	OGLE, this paper

Table A.1. continued.

Star	JD Hel.- 2 400 000	Error [day]	Epoch	Filter	Source Observatory
HV 982	56 257.56416	0.0001	1296.5	<i>I</i>	DK154, this paper
HV 982	56 257.56421	0.0001	1296.5	<i>I</i>	DK154, this paper
HV 982	56 265.71152	0.0001	1298.0	<i>I</i>	DK154, this paper
HV 982	56 265.71137	0.0001	1298.0	<i>I</i>	DK154, this paper
HV 982	56 297.72209	0.0003	1304.0	<i>I</i>	DK154, this paper
HV 982	56 297.72347	0.0003	1304.0	<i>I</i>	DK154, this paper
HV 2274	13 875.807		-5977.0		Gaposhkin (1977)
HV 2274	23 486.545		-4298.5		Gaposhkin (1977)
HV 2274	23 638.498		-4272.0		Gaposhkin (1977)
HV 2274	23 732.679		-4255.5		Gaposhkin (1977)
HV 2274	26 246.582		-3816.5		Gaposhkin (1977)
HV 2274	26 710.335		-3735.5		Gaposhkin (1977)
HV 2274	26 956.619		-3692.5		Gaposhkin (1977)
HV 2274	27 801.283		-3545.0		Gaposhkin (1977)
HV 2274	30 589.627		-3058.0		Gaposhkin (1977)
HV 2274	31 299.629		-2934.0		Gaposhkin (1977)
HV 2274	31 740.496		-2857.0		Gaposhkin (1977)
HV 2274	32 058.690		-2801.5		Gaposhkin (1977)
HV 2274	32 347.570		-2751.0		Gaposhkin (1977)
HV 2274	32 891.428		-2656.0		Gaposhkin (1977)
HV 2274	32 940.457		-2647.5		Gaposhkin (1977)
HV 2274	48 099.818		0.0		Watson et al. (1992)
HV 2274	48 102.817		0.5		Watson et al. (1992)
HV 2274	48 827.0456		127.0		MP05
HV 2274	48 829.988		127.5		MP05
HV 2274	48 947.28675	0.01254	148.0	<i>B</i>	MACHO, this paper
HV 2274	48 950.23969	0.01483	148.5	<i>B</i>	MACHO, this paper
HV 2274	49 136.25131	0.00567	181.0	<i>B</i>	MACHO, this paper
HV 2274	49 139.18771	0.01070	181.5	<i>B</i>	MACHO, this paper
HV 2274	49 359.56433	0.00636	220.0	<i>B</i>	MACHO, this paper
HV 2274	49 362.49934	0.00401	220.5	<i>B</i>	MACHO, this paper
HV 2274	49 499.9047		244.5		MP05
HV 2274	49 502.7137		245.0		MP05
HV 2274	49 614.42969	0.00578	264.5	<i>B</i>	MACHO, this paper
HV 2274	49 617.24018	0.00664	265.0	<i>B</i>	MACHO, this paper
HV 2274	49 889.2576		312.5		MP05
HV 2274	49 892.104		313.0		MP05
HV 2274	49 906.44901	0.01254	315.5	<i>B</i>	MACHO, this paper
HV 2274	49 909.28085	0.01763	316.0	<i>B</i>	MACHO, this paper
HV 2274	50 287.19199	0.00452	382.0	<i>B</i>	MACHO, this paper
HV 2274	50 290.07136	0.00767	382.5	<i>B</i>	MACHO, this paper
HV 2274	50 659.39741	0.00515	447.0	<i>B</i>	MACHO, this paper
HV 2274	50 662.24002	0.00425	447.5	<i>B</i>	MACHO, this paper
HV 2274	50 957.1546		499.0		MP05
HV 2274	50 959.971		499.5		MP05
HV 2274	51 214.82801	0.00315	544.0	<i>B</i>	MACHO, this paper
HV 2274	51 217.64304	0.00527	544.5	<i>B</i>	MACHO, this paper
HV 2274	52 445.93977	0.00596	759.0	<i>I</i>	OGLE, this paper
HV 2274	52 448.67936	0.01065	759.5	<i>I</i>	OGLE, this paper
HV 2274	52 998.35630	0.00504	855.5	<i>I</i>	OGLE, this paper
HV 2274	53 001.37141	0.00431	856.0	<i>I</i>	OGLE, this paper
HV 2274	53 528.17437	0.00624	948.0	<i>I</i>	OGLE, this paper
HV 2274	53 530.84233	0.00424	948.5	<i>I</i>	OGLE, this paper
HV 2274	54 069.07211	0.01346	1042.5	<i>I</i>	OGLE, this paper
HV 2274	54 072.15199	0.01866	1043.0	<i>I</i>	OGLE, this paper
HV 2274	54 469.86569	0.02703	1112.5	<i>I</i>	OGLE, this paper
HV 2274	54 472.97310	0.01248	1113.0	<i>I</i>	OGLE, this paper
HV 2274	54 819.14866	0.00470	1173.5	<i>I</i>	OGLE, this paper
HV 2274	54 822.26597	0.00618	1174.0	<i>I</i>	OGLE, this paper
HV 2274	56 204.78877	0.00079	1415.5	<i>R</i>	DK154, this paper
HV 2274	56 267.77936	0.00267	1426.5	<i>R</i>	DK154, this paper
HV 2274	56 270.95500	0.00257	1427.0	<i>R</i>	DK154, this paper
HV 2274	56 299.58505	0.00231	1432.0	<i>R</i>	DK154, this paper
HV 2274	56 290.67754	0.00178	1430.5	<i>R</i>	DK154, this paper

Table A.1. continued.

Star	JD Hel.- 2 400 000	Error [day]	Epoch	Filter	Source Observatory
MACHO 78.6097.13	48 968.15382	0.00342	-1112.5	<i>BR</i>	MACHO, this paper
MACHO 78.6097.13	48 969.63869	0.00206	-1112.0	<i>BR</i>	MACHO, this paper
MACHO 78.6097.13	49 201.18083	0.00205	-1037.5	<i>BR</i>	MACHO, this paper
MACHO 78.6097.13	49 202.66301	0.00385	-1037.0	<i>BR</i>	MACHO, this paper
MACHO 78.6097.13	49 431.10223	0.00306	-963.5	<i>BR</i>	MACHO, this paper
MACHO 78.6097.13	49 432.57665	0.00549	-963.0	<i>BR</i>	MACHO, this paper
MACHO 78.6097.13	49 631.43145	0.00707	-899.0	<i>BR</i>	MACHO, this paper
MACHO 78.6097.13	49 633.06235	0.00284	-898.5	<i>BR</i>	MACHO, this paper
MACHO 78.6097.13	49 855.13418	0.00370	-827.0	<i>BR</i>	MACHO, this paper
MACHO 78.6097.13	49 856.77458	0.00531	-826.5	<i>BR</i>	MACHO, this paper
MACHO 78.6097.13	50 106.80963	0.00559	-746.0	<i>BR</i>	MACHO, this paper
MACHO 78.6097.13	50 108.44539	0.00551	-745.5	<i>BR</i>	MACHO, this paper
MACHO 78.6097.13	50 305.65322	0.00573	-682.0	<i>BR</i>	MACHO, this paper
MACHO 78.6097.13	50 307.29116	0.00378	-681.5	<i>BR</i>	MACHO, this paper
MACHO 78.6097.13	50 557.32252	0.00262	-601.0	<i>BR</i>	MACHO, this paper
MACHO 78.6097.13	50 558.96600	0.00634	-600.5	<i>BR</i>	MACHO, this paper
MACHO 78.6097.13	50 801.31406	0.00683	-522.5	<i>BR</i>	MACHO, this paper
MACHO 78.6097.13	50 802.77817	0.00996	-522.0	<i>BR</i>	MACHO, this paper
MACHO 78.6097.13	51 231.54291	0.00308	-384.0	<i>BR</i>	MACHO, this paper
MACHO 78.6097.13	51 233.18484	0.00640	-383.5	<i>BR</i>	MACHO, this paper
MACHO 78.6097.13	52 424.64757	0.00294	0.0	<i>I</i>	OGLE, this paper
MACHO 78.6097.13	52 426.28805	0.00233	0.5	<i>I</i>	OGLE, this paper
MACHO 78.6097.13	52 993.24107	0.00798	183.0	<i>I</i>	OGLE, this paper
MACHO 78.6097.13	52 994.86101	0.00267	183.5	<i>I</i>	OGLE, this paper
MACHO 78.6097.13	53 524.54977	0.00558	354.0	<i>I</i>	OGLE, this paper
MACHO 78.6097.13	53 523.05361	0.00298	353.5	<i>I</i>	OGLE, this paper
MACHO 78.6097.13	54 270.23860	0.00578	594.0	<i>I</i>	OGLE, this paper
MACHO 78.6097.13	54 271.83416	0.00167	594.5	<i>I</i>	OGLE, this paper
MACHO 78.6097.13	54 782.91373	0.00432	759.0	<i>I</i>	OGLE, this paper
MACHO 78.6097.13	54 784.48892	0.00370	759.5	<i>I</i>	OGLE, this paper
MACHO 78.6097.13	56 314.70125	0.00179	1252.0	<i>R</i>	DK154, this paper
MACHO 81.8881.47	49 151.63566	0.0005	-0.5		MP05
MACHO 81.8881.47	49 153.34993	0.0005	0.0		MP05
MACHO 81.8881.47	49 392.29958	0.0005	61.5		MP05
MACHO 81.8881.47	49 394.04567	0.0005	62.0		MP05
MACHO 81.8881.47	49 790.01510	0.0005	164.0		MP05
MACHO 81.8881.47	49 792.12920	0.0005	164.5		MP05
MACHO 81.8881.47	50 170.45366	0.0005	262.0		MP05
MACHO 81.8881.47	50 172.52273	0.0005	262.5		MP05
MACHO 81.8881.47	50 341.26363	0.0005	306.0		MP05
MACHO 81.8881.47	50 343.32028	0.0005	306.5		MP05
MACHO 81.8881.47	50 987.69498	0.0005	472.5		MP05
MACHO 81.8881.47	50 989.55366	0.0005	473.0		MP05
MACHO 81.8881.47	51 003.19013	0.0005	476.5		MP05
MACHO 81.8881.47	51 005.07908	0.0005	477.0		MP05
MACHO 81.8881.47	51 581.55557	0.0005	625.5		MP05
MACHO 81.8881.47	51 583.49576	0.0005	626.0		MP05
MACHO 81.8881.47	52 291.91465	0.0091	808.5	<i>I</i>	OGLE, this paper
MACHO 81.8881.47	52 293.91729	0.0037	809.0	<i>I</i>	OGLE, this paper
MACHO 81.8881.47	52 635.53595	0.0052	897.0	<i>I</i>	OGLE, this paper
MACHO 81.8881.47	52 637.38335	0.0877	897.5	<i>I</i>	OGLE, this paper
MACHO 81.8881.47	53 184.70263	0.0163	1038.5	<i>I</i>	OGLE, this paper
MACHO 81.8881.47	53 186.77939	0.1164	1039.0	<i>I</i>	OGLE, this paper
MACHO 81.8881.47	53 912.70392	0.0052	1226.0	<i>I</i>	OGLE, this paper
MACHO 81.8881.47	53 914.45626	0.0034	1226.5	<i>I</i>	OGLE, this paper
MACHO 81.8881.47	54 485.06658	0.0014	1373.5	<i>I</i>	OGLE, this paper
MACHO 81.8881.47	54 487.25375	0.0049	1374.0	<i>I</i>	OGLE, this paper
MACHO 81.8881.47	54 830.54160	0.0042	1462.5	<i>I</i>	OGLE, this paper
MACHO 81.8881.47	54 832.75781	0.0124	1463.0	<i>I</i>	OGLE, this paper
MACHO 81.8881.47	56 284.61939	0.0008	1837.0	<i>R</i>	DK154, this paper
MACHO 81.8881.47	56 332.75573	0.0010	1849.5	<i>R</i>	DK154, this paper
MACHO 79.5377.76	48 965.66934	0.00419	-1250.5	<i>R</i>	MACHO, this paper
MACHO 79.5377.76	48 966.92100	0.00198	-1250.0	<i>R</i>	MACHO, this paper

Table A.1. continued.

Star	JD Hel.- 2 400 000	Error [day]	Epoch	Filter	Source Observatory
MACHO 79.5377.76	49 197.69453	0.00124	-1162.5	<i>R</i>	MACHO, this paper
MACHO 79.5377.76	49 198.94037	0.00551	-1162.0	<i>R</i>	MACHO, this paper
MACHO 79.5377.76	49 452.04656	0.00129	-1066.0	<i>R</i>	MACHO, this paper
MACHO 79.5377.76	49 453.44570	0.00382	-1065.5	<i>R</i>	MACHO, this paper
MACHO 79.5377.76	49 702.52111	0.00264	-971.0	<i>R</i>	MACHO, this paper
MACHO 79.5377.76	49 703.92184	0.00163	-970.5	<i>R</i>	MACHO, this paper
MACHO 79.5377.76	49 951.76191	0.00140	-876.5	<i>R</i>	MACHO, this paper
MACHO 79.5377.76	49 950.35515	0.00235	-877.0	<i>R</i>	MACHO, this paper
MACHO 79.5377.76	50 177.10012	0.00171	-791.0	<i>R</i>	MACHO, this paper
MACHO 79.5377.76	50 178.51120	0.00206	-790.5	<i>R</i>	MACHO, this paper
MACHO 79.5377.76	50 356.38361	0.00169	-723.0	<i>R</i>	MACHO, this paper
MACHO 79.5377.76	50 355.15816	0.00177	-723.5	<i>R</i>	MACHO, this paper
MACHO 79.5377.76	50 626.72815	0.00113	-620.5	<i>R</i>	MACHO, this paper
MACHO 79.5377.76	50 627.95207	0.00272	-620.0	<i>R</i>	MACHO, this paper
MACHO 79.5377.76	50 952.24739	0.00722	-497.0	<i>R</i>	MACHO, this paper
MACHO 79.5377.76	50 951.03095	0.04825	-497.5	<i>R</i>	MACHO, this paper
MACHO 79.5377.76	51 324.00854	0.00419	-356.0	<i>R</i>	MACHO, this paper
MACHO 79.5377.76	51 325.41971	0.00198	-355.5	<i>R</i>	MACHO, this paper
MACHO 79.5377.76	52 447.20093	0.00156	70.0	<i>I</i>	OGLE, this paper
MACHO 79.5377.76	52 445.95855	0.00132	69.5	<i>I</i>	OGLE, this paper
MACHO 79.5377.76	52 994.36017	0.00348	277.5	<i>I</i>	OGLE, this paper
MACHO 79.5377.76	52 992.97769	0.00256	277.0	<i>I</i>	OGLE, this paper
MACHO 79.5377.76	53 354.19440	0.00556	414.0	<i>I</i>	OGLE, this paper
MACHO 79.5377.76	53 352.92752	0.01318	413.5	<i>I</i>	OGLE, this paper
MACHO 79.5377.76	53 892.06597	0.00182	618.0	<i>I</i>	OGLE, this paper
MACHO 79.5377.76	53 893.41737	0.00150	618.5	<i>I</i>	OGLE, this paper
MACHO 79.5377.76	54 522.21822	0.00205	857.0	<i>I</i>	OGLE, this paper
MACHO 79.5377.76	54 520.91151	0.00071	856.5	<i>I</i>	OGLE, this paper
MACHO 79.5377.76	54 833.34419	0.00145	975.0	<i>I</i>	OGLE, this paper
MACHO 79.5377.76	54 832.01969	0.00063	974.5	<i>I</i>	OGLE, this paper
MACHO 79.5377.76	56 315.12485	0.005	1537.0	<i>R</i>	DK154, this paper
MACHO 79.5377.76	56 383.67777	0.00040	1563.0	<i>R</i>	DK154, this paper

Appendix B: Table of radial velocities

Table B.1. List of the radial velocities used for the analysis.

Star	JD Hel.- 2 400 000	RV_1 [km s ⁻¹]	RV_2 [km s ⁻¹]
MACHO 81.8881.47	52 243.62965	197.825	344.054
MACHO 81.8881.47	52 243.69480	169.847	374.850
MACHO 81.8881.47	52 243.77655	157.162	397.739
MACHO 81.8881.47	52 246.54851	430.591	119.457
MACHO 81.8881.47	52 257.64245	376.268	169.630
MACHO 81.8881.47	52 270.74072	208.679	322.865
MACHO 81.8881.47	52 289.69123	376.342	169.518
MACHO 81.8881.47	52 294.58185	137.413	418.659
MACHO 81.8881.47	52 320.67094	391.611	143.591
MACHO 79.5377.76	52 214.79259	58.559	440.768
MACHO 79.5377.76	52 226.72978	415.303	94.430
MACHO 79.5377.76	52 243.72257	38.347	451.361
MACHO 79.5377.76	52 244.58815	415.863	77.425
MACHO 79.5377.76	52 244.70911	441.078	54.155
MACHO 79.5377.76	52 245.81943	121.623	372.537
MACHO 79.5377.76	52 246.60116	125.476	371.131
MACHO 79.5377.76	52 270.69835	325.508	177.316
MACHO 79.5377.76	52 270.76503	352.081	147.711
MACHO 79.5377.76	52 271.61223	387.922	115.153
MACHO 79.5377.76	52 271.63592	373.100	124.104
MACHO 79.5377.76	52 296.59889	91.741	409.521
MACHO 79.5377.76	52 309.54136	36.136	470.775
MACHO 79.5377.76	52 309.57452	31.116	476.893